Citation
Sheppard, D.A. and Jepsen, L.H. and Rowles, M.R. and Paskevicius, M. and Jensen, T.R. and Buckley, C.E. 2019. Decomposition pathway of KAlH4 altered by the addition of Al2S3. Dalton Transactions. 48 (15): pp. 5048-5057. http://doi.org/10.1039/c9dt00457b

ARTICLE

Decomposition pathway of $KAlH_4$ altered by the addition of Al_2S_3

Drew A. Sheppard,*[a] Lars H. Jepsen,[b,c] Matthew R. Rowles,[a,d] Mark Paskevicius,[a] Torben R. Jensen [b] and Craig E. Buckley [a]

Received 00th January 20xx,
Accepted 00th January 20xx

DOI: 10.1039/x0xx00000x

Altering the decomposition pathway of a potassium alanate, $KAlH_4$, with aluminium sulfide, Al_2S_3, presents a new opportunity to release all of the hydrogen, increase the volumetric hydrogen capacity and avoid complications associated with the formation of KH and molten K. Decomposition of $6KAlH_4$-Al_2S_3 during heating under dynamic vacuum began at 185 °C, 65 °C lower than for pure $KAlH_4$, and released 71% of the theoretical hydrogen content below 300 °C via several unknown compounds. The major hydrogen release event, centred at 276 °C, was associated with two new compounds indexed with monoclinic (a = 10.505, b = 7.492, c = 11.772 Å, β = 122.88°) and hexagonal (a = 10.079, c = 7.429 Å) unit cells, respectively. Unlike the $6NaAlH_4$-Al_2S_3 system, the $6KAlH_4$-Al_2S_3 system did not have M_3AlH_6 (M = alkali metal) as one of the intermediate decomposition products nor were the final products M_2S and Al observed. Decomposition performed under hydrogen pressure initially followed a similar reaction pathway to that observed during heating under vacuum but resulted in partial melting of the sample between 300 and 350 °C. The measured enthalpy of hydrogen absorption (ΔH_{abs}) was in the range -44.5 to -51.1 kJ/mol·H_2, which is favourable for moderate temperature hydrogen applications. Although, the hydrogen capacity decrease during consecutive H_2 release and uptake cycles, the presence of excess amounts of aluminium allow for further optimisation hydrogen storage properties.

Introduction

Storing hydrogen in a safe, compact and efficient manner is a barrier to its widespread use as an energy carrier. Hydrogen can be stored in the solid state as metal hydrides, which incorporate classes of compounds such as: simple saline hydrides (e.g. NaH, MgH_2 etc); metallic and intermetallic hydrides of transition metals (e.g. $LaNi_5H_6$, TiH_2) and; complex hydrides, such as alanates (anions of AlH_4^- or AlH_6^{3-}), amides/imides (anions of NH_2^- or NH^{2-}) and borohydrides (anions of BH_4^-). [1-8] One of the attractions of complex metal hydrides, in particular, is that they readily undergo cation and anion substitution[9] which provides an easy means of altering their properties. As a result, complex metal hydrides are now being investigated as solid-state electrolytes,[10-12] high-capacity anodes in batteries,[12-16] photovoltaic materials,[17] magnetic refrigeration materials[18] and luminescent materials for optoelectronic applications.[19]

However, interest in metal hydrides extends far beyond the challenging requirements of hydrogen storage for fuel-cell vehicles and includes their use as thermal storage materials for concentrating solar power plants [20-31] and as hydrogen storage materials for stationary fuel cells [5, 16, 32-34]. Recent research into metal hydrides now extends well beyond their ability to store hydrogen and includes exploring their potential in a wide range of energy related applications based on a number of unique, unexpected and only recently discovered properties [4, 17, 35]. The potential of using metal sulphides as solid-state electrolytes [36, 37], as cathode materials in metal-sulphur batteries [38] and as heterogeneous catalysts [39-41], means the interest in the $KAlH_4$-Al_2S_3 system extends beyond just its potential for hydrogen storage. The discovery of new sulphur containing hydride phases provides potential for a rich new area of materials research. Determination of the hydrogen bonding environment in these compounds may lead to the design and optimisation of new materials. For example, research on the interaction between alkali metal borohydrides and pure sulphur [42] has led to the development of solution-stable sulphurated borohydrides, such as $NaBH_2S_3$ [43] and $Ca(BH_2S_3)_2$,[44] as selective reducing agents for organic syntheses. Investigation of the destabilisation of $KAlH_4$ by Al_2S_3 is a step along this path to new sulphur containing hydride phases with novel properties.

Alanates of light alkali metals (M = Li or Na) release hydrogen in a multistep process, Equation 1 - 3.

$$3MAlH_4 \leftrightarrow M_3AlH_6 + 2Al + 3H_2 \quad (1)$$

$$M_3AlH_6 \leftrightarrow 3MH + Al + 1.5H_2 \quad (2)$$

$$3MH \leftrightarrow 3M + 1.5\ H_2 \quad (3)$$

However, the thermodynamic properties of $KAlH_4$ and its decomposition pathways are less straightforward. The reported experimental enthalpy, H_f^o, of $KAlH_4$ varies between -167.0 kJ/mol [45, 46] and -183.7 kJ/mol [47] while the entropy, S^o, has been reported as 129 J/mol·H_2·K [46] and 112.9 J/mol·H_2·K [48], respectively. Even the exact decomposition pathway of $KAlH_4$

[a] Hydrogen Storage Research Group, Fuels and Energy Technology Institute, Department of Physics and Astronomy, Curtin University, GPO Box U1987, Perth, WA 6845, Australia.
[b] Interdisciplinary Nanoscience Center (iNANO) and Department of Chemistry, University of Aarhus, DK-8000, Denmark.
[c] Danish Technological Institute, Kongsvang Alle 29, 8000 Aarhus, Denmark.
[d] John de Laeter Centre, Curtin University, GPO Box U1987, Perth, WA, 6845, Australia.

Electronic Supplementary Information (ESI) available: Further X-ray diffraction and gas measurement data. See DOI: 10.1039/x0xx00000x

has not been fully clarified. Techniques that employed variable temperature, such as differential scanning calorimetry [49] or *in situ* synchrotron X-ray diffraction,[50] showed that it did not decompose via the hexalanate, M_3AlH_6, like the lighter alkali metals. However, $KAlH_4$ investigated at constant temperature, using pressure-composition-isotherm measurements, showed two pressure plateaux [51] consistent with the two-step decomposition process of Eq. 1 and Eq. 2.

Sodium alanate, $NaAlH_4$, is thermodynamically destabilised by its reaction with Al_2S_3, showing promising kinetics and hydrogen reversibility without a catalyst [52]. The reaction in the system $6NaAlH_4$-Al_2S_3 was predicted using thermodynamic software to be a single-step process forming Na_2S and Al. However, detailed experimental investigations reveal that the reaction between $NaAlH_4$ and Al_2S_3 followed a complex multi-step decomposition pathway [46].

Here we extend our investigations to include potassium aluminium alanate, i.e. $6KAlH_4$-Al_2S_3, which could potentially have a hydrogen capacity of 4.2 wt% and a volumetric hydrogen capacity of 58.5 kg H_2/m^3. This still compares well to pure $KAlH_4$, i.e. ρ_m = 4.3 wt% and ρ_V = 53.4 kg H_2/m^3.

Experimental

Synthesis

All handling and storage of chemicals was performed in argon-filled glove-boxes equipped with circulation purifiers. Sample preparation: Small chunks of Al_2S_3 (98%, Sigma-Aldrich) were ball milled using a Fritz Pulveritsette 4 planetary ball mill, a tungsten carbide (WC) vial (80 mL) and 10 mm diameter balls in a ball-to-powder (BTP) mass ratio of 15:1. The powder was ball-milled at 300 rpm for 2 min followed by a 2 min break with this sequence repeated 60 times. Synthesis of $KAlH_4$ was performed as reported previously.[50] Briefly, potassium hydride, KH, 30 wt% dispersion in oil (Sigma-Aldrich) was washed and filtered with diethyl ether and dried. Aluminium powder (99.99 %, Sigma-Aldrich) and dried KH (1:1 molar ratio) were ball milled using a Fritz Pulveritsette 4 planetary ball mill, a WC vial (80 mL) and 10 mm diameter balls in a BTP ratio of 30:1. The powder was ball-milled at 380 rpm for 5 min intervened by a 2 min break and this sequence was repeated 24 times. The ball-milled powder was subsequently heated at 270 °C for 59 h in hydrogen, $p(H_2)$ = 175 bar. $KAlH_4$-Al_2S_3 (6:1 molar ratio) was ball-milled at 250 rpm for 2 min followed by a 2 min break with this sequence repeated 60 times using a Fritz Pulveritsette 6 planetary ball mill, a WC vial (80 mL) and 10 mm diameter balls in a BTP ratio of 15:1. The XRD patterns of the Al_2S_3 starting reagent and the ball-milled $6KAlH_4$-Al_2S_3 are also included in Figure S1. Note that the milling vial and balls can introduce minor quantities of WC into the samples.

Characterisation

In situ Synchrotron X-ray Diffraction (in situ SXRD): In situ SXRD data was collected at Beamline I711 at the MAX-II synchrotron in the research laboratory MAX-lab, Lund, Sweden with a MAR165 CCD detector system. The samples were packed in a sapphire (Al_2O_3) single-crystal tube (1.09 mm o.d., 0.79 mm i.d.) using a specially designed sample holder [53]. The wavelength employed was λ = 0.9941 Å for pure $KAlH_4$ and 0.9904 Å for both $6KAlH_4$-Al_2S_3 samples. The heating rates used were 6.4 °C/min for pure $KAlH_4$ heated under vacuum, 7.1 °C/min for $6KAlH_4$-Al_2S_3 heated under vacuum and 4.9 °C/min for $6KAlH_4$-Al_2S_3 heated under 7 bar of H_2 pressure. All patterns, including the *ex situ* ones collected with the laboratory-based instrument, were converted to q-range for ease of comparison. The relation between direct space (ϑ and d) and reciprocal space (q) are $q = 4\pi\sin(\vartheta)/\lambda$, where 2ϑ is the scattering angle, and $q = 2\pi/d$, respectively. All *in situ* data contains a large sloping background originating from the capillaries. To improve visual clarity, the background scattering of the room temperature pattern was fitted and subtracted from each *in situ* data set and the intensities were plotted on a logarithmic scale. High-resolution data were also collected for a sample of $6KH$-Al_2S_3 at the Swiss-Norwegian Beamline (SNBL), ESRF, Grenoble, France, with a Pilatus area detector using a wavelength of λ = 0.68134 Å. This sample was used to index the major unknown phases seen during $6KAlH_4$-Al_2S_3 decomposition. Diffracted Intensities from individual compounds are extracted qualitatively from well resolved, selected Bragg peaks.

Ex situ Laboratory-based X-ray Diffraction (ex situ XRD): Ex-situ XRD patterns of $KAlH_4$ and hydrogen cycled $6KAlH_4$-Al_2S_3 were measured on a Rigaku Smart Lab diffractometer using a Cu source and a parallel beam multilayer mirror (Cu Kα1 radiation, λ = 1.540593 Å). Data were collected in the 2θ-range 10 to 60°. All air-sensitive samples were mounted in 0.5 mm glass capillaries sealed with epoxy within a glove-box.

Temperature Programmed Desorption Mass Spectrometry (TPD-MS): TPD-MS was performed on two samples: pure $KAlH_4$ and $KAlH_4$ - Al_2S_3 (6:1 molar ratio) at a heating rate of, $\Delta T/\Delta t$ = 5 °C/min. The samples (approx. 5 mg) were placed in an Al crucible and heated from 50 to 500 °C ($\Delta T/\Delta t$ = 5 °C/min) in an argon flow of 20 mL/min. The gaseous species released during thermal ramping were analysed for release of H_2 (and H_2S for the sulphur containing phases) by a Hiden Analytical HPR-20 QMS sampling system. Hydrogen was the only detectable gas in TPD-MS measurements and no H_2S release (m/z = 34) was recorded unless samples were first exposed to air/moisture.

Sieverts Data: Hydrogen desorption/absorption measurements were undertaken on custom built Sieverts instrument. Pressure was monitored using Rosemount 3051S pressure transducers and sample temperature was monitored internally using a K-type thermocouple. The ambient volume and temperature of the Sieverts instrument was ~27 cm^3 and ~27 °C, respectively while the non-ambient volume of the sample reactor was ~5 cm^3. Approximately 50 - 100 mg of $6KAlH_4$-Al_2S_3 was heated

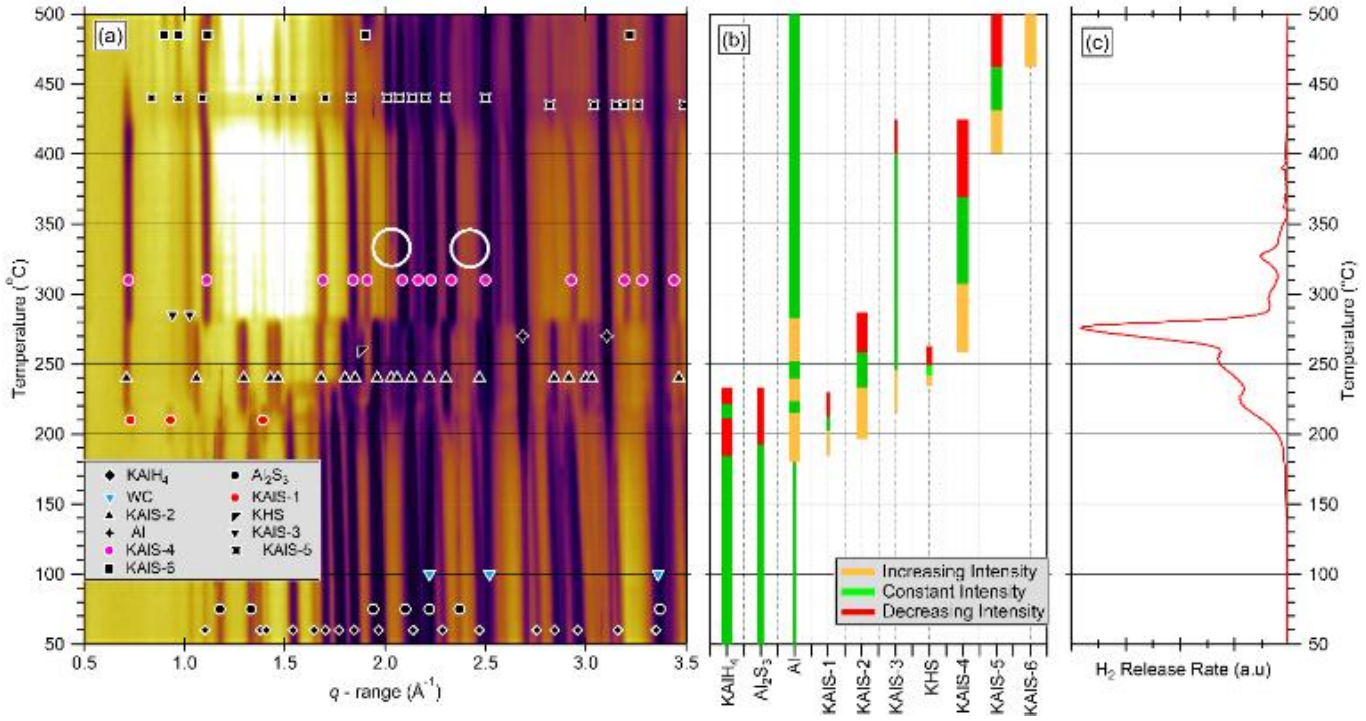

Figure 1: (a) *In situ* SXRD data of 6KAlH$_4$ - Al$_2$S$_3$ performed under vacuum ($\Delta T/\Delta t$ = 7.1 °C/min), (b) summary of sample composition as a function of temperature extracted from the *in situ* SR-XRD data where bar widths are a qualitative indicator of phase fractions. (c) Hydrogen release measured by TPD-MS (m/e = 2) of 6KAlH$_4$-Al$_2$S$_3$ ($\Delta T/\Delta t$ = 5 °C/min).

from RT to 515 °C ($\Delta T/\Delta t$ = 5 °C/min) and then the temperature was kept constant at 515 °C for between 20 mins and 4 h under the evolved hydrogen pressure that varied between ~0.5 and ~1.5 bar depending on the sample mass and degree of rehydrogenation. Rehydrogenation was undertaken by loading a volume with 400 bar of H_2 at RT and then performing an isothermal absorption at 300 °C for 6 hours (pressure ~430 bar).

Temperature Programmed Photographic Analysis (TPPA): TPPA [54-58] was performed using a digital camera and a specially designed sample holder whilst heating the sample at, $\Delta T/\Delta t$ = 3 °C/min from RT to 500 °C. A sample of 6KAlH$_4$-Al$_2$S$_3$ was sealed under argon in a glass vial connected to a 1 bar blow-off valve to maintain atmospheric pressure. A thermocouple was in contact with the sample within the glass vial to monitor temperature during heating. To examine the effect of hydrogen back-pressure on the system, a second sample of 6KAlH$_4$-Al$_2$S$_3$ was sealed under a H_2 pressure of ~4 bar at room temperature and heated at $\Delta T/\Delta t$ = 5 °C/min. This H_2 pressure increased to ~9 bar by the time the sample reached 430 °C. The glass vial was encased within an aluminium block with open viewing windows for photography, to provide near-uniform heating by rod heaters, interfaced to a temperature controller.

Safety warning: Handling of these samples comprises a number of safety hazards. KAlH$_4$ reacts violently with water and may spontaneously combust in air. The presence of trace amounts of metallic K or KH in KAlH$_4$ and its decomposition products can form explosive potassium superoxides that may detonate with minor friction or heat. It is recommended that KH, KAlH$_4$ and K$_3$AlH$_6$ should be synthesised fresh when needed, stored under stringent inert atmosphere conditions, not stored in the decomposed state, and that any excess solid should be destroyed immediately after use [50, 59]. Exposure of Al$_2$S$_3$ (and metal sulfides in general) to water or atmospheric moisture can release toxic hydrogen sulphide gas, H_2S.

Results and Discussion

Characterisation of 6KAlH$_4$ - Al$_2$S$_3$ decomposed under vacuum

In situ SXRD and TPD-MS measurements were performed on pure KAlH$_4$ and the results are shown in Figure S2 while selected diffraction patterns are shown in Figure S3. The observed decomposition for KAlH$_4$ was similar to previous investigations [50] and involve three unknown compounds, henceforth referred to as PK-1, PK-2 and PK-3, in addition to Al and KH (see Figure S2b).

In situ SXRD patterns collected under vacuum during heating of 6KAlH$_4$-Al$_2$S$_3$ and corresponding sample composition analysis and TPD-MS results are presented in Figure 1 (a), (b) and (c), respectively. Individual SXRD patterns for selected temperatures are presented in the supporting information, Figure S4. The *in situ* SXRD data, Figure 1(a), shows that there are 6 unidentifiable compounds (referred to as KAlS-1 to KAlS-6, respectively) that occur between 184 and 500 °C associated with the reaction between KAlH$_4$ and Al$_2$S$_3$ and that the high-temperature cubic polymorph of KHS [60, 61] also briefly exists between 235 and 263 °C. The unknown phases do not correspond to those observed during *in situ* SXRD decomposition of pure KAlH$_4$ nor do they correspond to any known combination of K, Al and S including K$_2$S, dipotassium polysulphides, Al$_2$S$_3$ polymorphs, KAlS$_2$ or K$_2$S.10Al$_2$S$_3$.[62]

TPD-MS of 6KAlH$_4$-Al$_2$S$_3$ is presented in Figure 1(c). Like the 6NaAlH$_4$-Al$_2$S$_3$ system [52], H_2 release from the 6KAlH$_4$-Al$_2$S$_3$

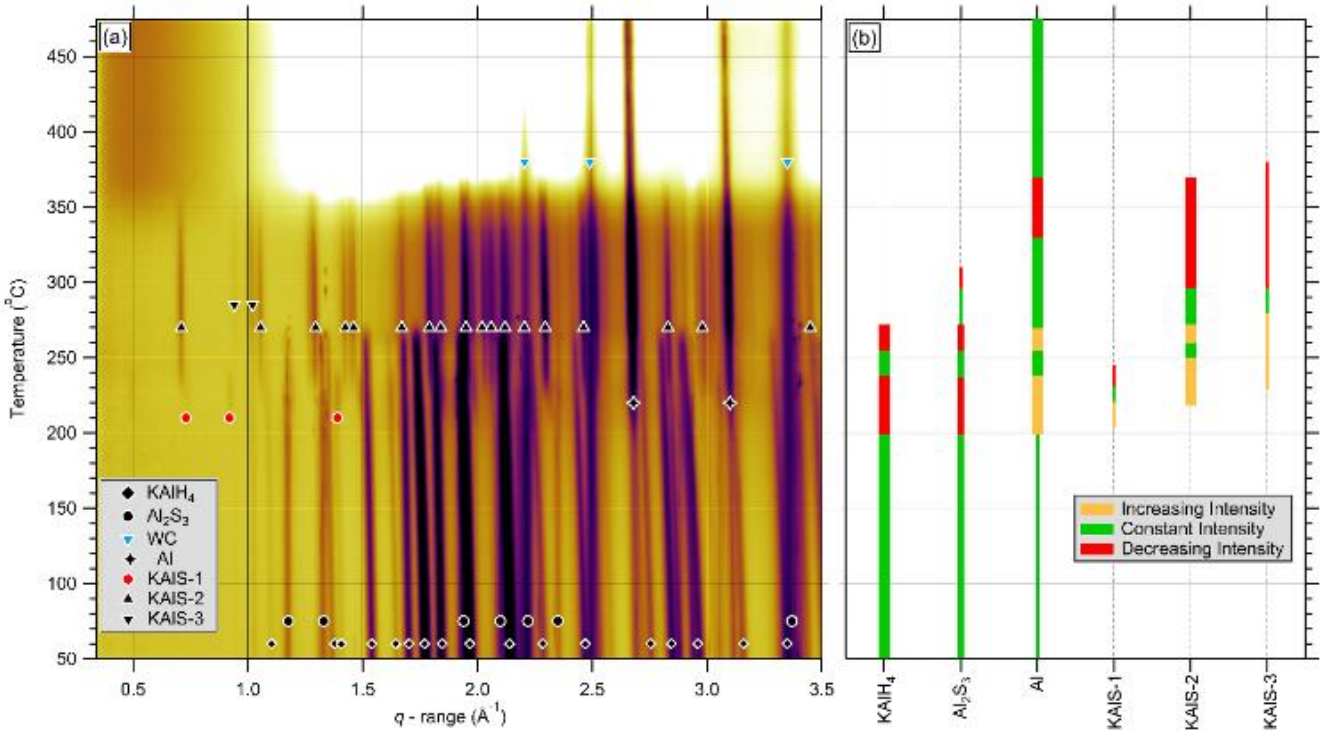

Figure 2: (a) *In situ* SXRD of 6KAlH$_4$-Al$_2$S$_3$ performed in $p(H_2)$ = 7 bar ($\Delta T/\Delta t$ = 4.9 °C/min) and; (b) sample composition as a function of temperature extracted from the *in situ* SXRD data (Figure 2a) where bar widths are a qualitative indicator of sample phase fractions.

system occurred in multiple steps with initial H_2 desorption beginning at ~180 °C,, which is ~70 °C lower than for pure $KAlH_4$. The maximum rate of H_2 release for the first desorption event occurred at 225 °C and corresponded to the consumption of the majority of the $KAlH_4$ and Al_2S_3 and the formation of KAlS-2. The second H_2 desorption event, centred at 253 °C in the TPD-MS, can be associated with the decomposition of KHS but, due to the resolution limitation and high degree of peak overlap, a decomposition product cannot readily be identified. The strongest TPD-MS H_2 desorption event, centred at 276 °C, corresponds to the decomposition of KAlS-2 and formation of KAlS-4. At the same time there was a noticeable decrease in the background scattering intensity between q ~ 1.2 - 1.65 Å^{-1}. Such background changes can often be associated with the changes in the crystallinity of a compound (e.g. amorphous solid ↔ crystalline solid or solid ↔ liquid transformation) [63]. The unknown compound KAlS-2 was indexed using TOPAS [64] in a monoclinic space group, $P21/c$, with lattice parameters of a = 10.505(3), b = 7.492(2), c = 11.772(3) Å and β = 122.88(2)° and V = 778.1(2) Å^3. KAlS-4 was indexed in hexagonal unit cell (space group $P31c$) with lattice parameters of a = 10.0787(3), c = 7.4294(4) Å and V = 653.57(3) Å^3.

TPD-MS, Figure 1(c), reveals that all of the H_2 is released from the sample below a temperature of 360 °C suggesting that the phases observed at temperatures above 360 °C only relate to solid-state reactions or phase transitions and not decomposition reactions. In particular, the formation mechanism of KAlS-5 can only be explained by one of two possibilities: (1) KAlS-5 forms as a reaction between the minor unknown phase KAlS-3 and the major unknown phase KAlS-4 since these both decrease concurrently or; (2) that KAlS-5 is the result of a solid-state phase transition from KAlS-4. Prior to the appearance of KAlS-5 at ~400°C, the KAlS-4 peaks at q values of ~ 2.928 and 3.193 Å^{-1} (d ~ 2.146 and 1.968 Å) undergo a sharp increase in q value in excess of that due to thermal expansion. At the same time, the peaks at q ~ 3.282 and 3.438 Å^{-1} (d ~ 1.914 and 1.828 Å) undergo a sharp decrease in q value that is in contradiction to their thermal expansion below 390 °C (selected data range of Figure 1 is enlarged in Figure S5). The Al peak intensities also stay constant during the formation of KAlS-5, which indicates that metallic Al is neither consumed nor produced.

By considering the *in situ* SXRD peak intensities in conjunction with TPD-MS data it is possible to conclude that the two major compounds, KAlS-2 and KAlS-4, are the primary ones involved with hydrogen release. This is similar to the 6NaAlH$_4$-Al$_2$S$_3$ where the hydrogen desorption reactions could primarily be attributed to only two compounds [52]. Two other major similarities were observed between the 6KAlH$_4$-Al$_2$S$_3$ and 6NaAlH$_4$-Al$_2$S$_3$ systems. The first was the fleeting appearance of the alkali hydrosulphide. In the potassium-based system, KHS existed in a ~30 °C temperature range that began from 235 °C while in the sodium-based system, NaHS existed in an ~18 °C temperature window that began at 140 °C. The second similarity was that both the potassium- and sodium-based system achieved the goal of releasing all of hydrogen contained within the samples at a lower temperature than the respective alkali metal alanates while avoiding the formation of the corresponding alkali metal hydrides and, subsequently, their molten alkali metals. The most significant difference between the alkali metal-based systems was that, unlike the sodium-based system, the final decomposition products in the

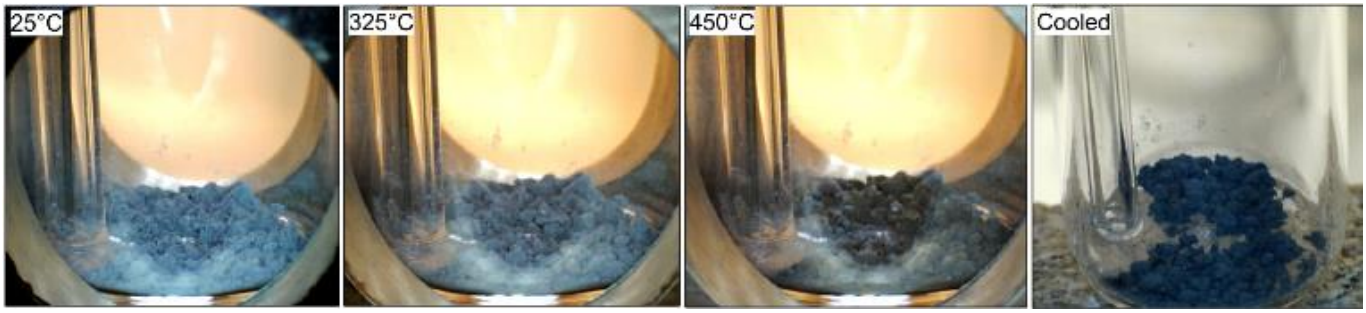

Figure 3: TPPA of $6KAlH_4$-Al_2S_3 heated in an initial argon pressure of 1 bar ($\Delta T/\Delta t$ = 3 °C/min).

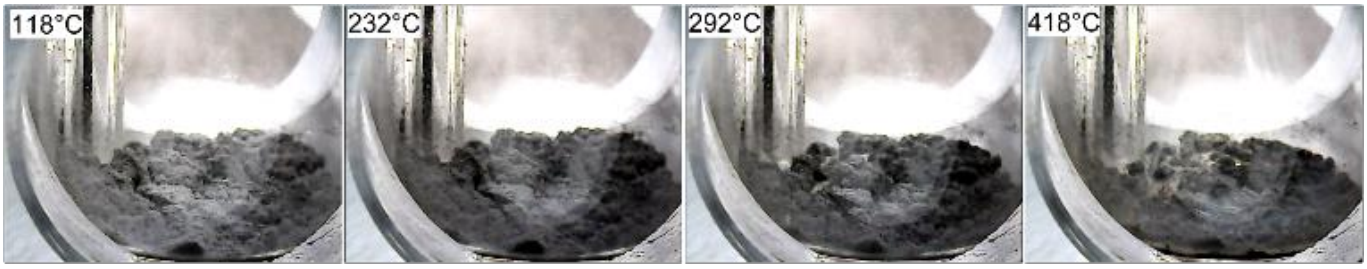

Figure 4: TPPA of $6KAlH_4$-Al_2S_3 heated under an initial H_2 pressure of 4 bar ($\Delta T/\Delta t$ = 5 °C/min).

potassium-based system were not the alkali metal sulphide, M_2S, and metallic Al. This would suggest a fundamental difference in relative stability of the compounds in the respective alkali metal-Al-S phase diagrams.

Characterisation of $6KAlH_4$-Al_2S_3 decomposed under H_2 pressure

The presence of a hydrogen back-pressure is known to change the decomposition pathway in some complex hydride systems [4]. For example, in $LiBH_4$ mixed with rare-earth hydrides a hydrogen back-pressure promotes the formation of the preferred metal boride during decomposition [65]. Thus, a hydrogen pressure during thermolysis can facilitate formation of metal borides, release of hydrogen and suppress release of diborane, B_2H_6 [66]. As such, the decomposition pathway of $6KAlH_4$-Al_2S_3 was examined by *in situ* SXRD during heating to 500 °C in $p(H_2)$ = 7 bar. The *in situ* SXRD data and the sample composition as a function of temperature are presented in Figure 2(a) and 2(b), respectively. Selected features of the *in situ* SXRD data at T > 350 °C are accentuated by a different colour scale in the supporting information, Figure S6(a), while individual SXRD patterns for selected temperatures are also presented in the supporting information, Figure S6(b).

There are some similarities as well as striking differences between the *in situ* SXRD data of $6KAlH_4$-Al_2S_3 heated at $p(H_2)$ = 7 bar compared to that heated under vacuum. The similarities include the initial phases that form, KAlS-1, KAlS-2 and KAlS-3, during reactions between $KAlH_4$ and Al_2S_3, but under H_2 pressure they form at higher in temperatures, ΔT ~ 30 °C, than they do under vacuum. The most dramatic difference is that for the sample heated at $p(H_2)$ = 7 bar, there is clear transition to a molten or amorphous state that begins slowly at ~320 °C and accelerates between 345 - 370 °C. Above q ~ 0.94 Å^{-1} (d = 1.06 Å) there is a pronounced decrease in the background intensity centred at q ~1.65 Å^{-1} (d = 3.81 Å) while below q ~ 0.94 Å^{-1} there is a pronounced increase in background intensity with a broad hump centred at q ~ 0.5 Å^{-1} (d = 12.57 Å). The hump centred at q ~ 0.5 Å^{-1} may be easier to see in the individual pattern presented in Figure S6(b). The d-spacing associated with this hump is substantially larger than that for molten potassium (q ~ 1.60 Å^{-1}, d = 3.93 Å) observed during the *in situ* heating of pure $KAlH_4$ and indicates that a different compound melted. After this event, the peak intensities of the impurity WC and Al are substantially reduced in intensity, most likely be attributed to some of the molten sample migrating out of the X-ray beam.

Temperature Programmed Photographic Analysis of $6KAlH_4$-Al_2S_3

To gain insight into the anomalous behaviour of the *in situ* SXRD sample heated under a back-pressure of H_2, TPPA analysis was performed on $6KAlH_4$-Al_2S_3 conducted in both argon and hydrogen atmosphere and images at selected temperatures are shown in Figure 3 and Figure 4, respectively. The full time lapse videos can be found in the supporting information. TPPA performed under argon showed only subtle volume changes in the powder sample before a gradual colour change from grey to black that began at ~360 °C and was complete by ~450 °C. TPPA performed under an initial H_2 pressure of ~4 bar (Figure 4) showed subtle changes with temperature. Between 260 and 292 °C, the sample showed a significant volume contraction that could be correlated to the two-step consumption of $KAlH_4$ and Al_2S_3 and formation of the unknown phases observed over a similar temperature range during *in situ* SXRD, Figure 2(a). A slow decrease in volume began between ~340 and 360 °C, accelerated between 360 and 400 °C, and then slowly continued up to a temperature of ~420 °C. These changes also mirrored those seen for the major phases, KAlS-2 and Al, observed during the corresponding *in situ* SXRD measurement.

Rehydrogenation Properties of $KAlH_4$-Al_2S_3

The $6KAlH_4$-Al_2S_3 was heated ($\Delta T/\Delta t$ = 5 °C/min) in an evacuated Sieverts instrument to assess the quantity of hydrogen released. During the first desorption, $6KAlH_4$-Al_2S_3 released 3.6

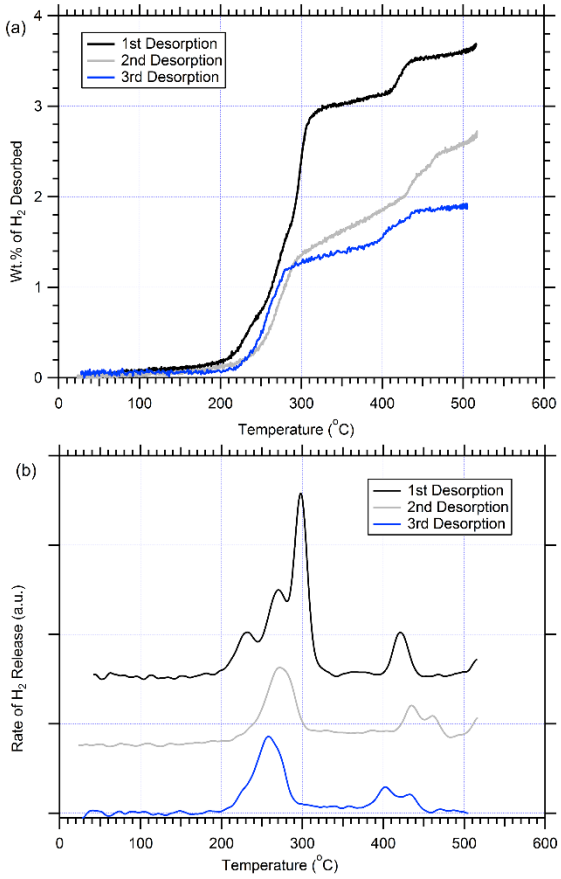

Figure 5: (a) Sieverts type measurement of gas release during heating of 6KAlH$_4$-Al$_2$S$_3$ ($\Delta T/\Delta t$ = 5 °C/min) showed as the equivalent amount of H$_2$ (wt%) desorbed over three consecutive cycles of hydrogen release and uptake and; (b) derivative of data in (a) that shows the rate of gas (H$_2$) release as a function of temperature.

wt% of H_2 before reaching 515 °C and another 0.3 wt% when held at this temperature for 4 hours, Figure 5(a). This corresponds to ~93% of the theoretical hydrogen content and falls within the practical capacity range observed for other metal hydrides. For example, 6NaAlH$_4$-Al$_2$S$_3$, NaMgH$_3$ and Mg$_2$FeH$_6$ [24, 52, 67] desorbed ~96%, ~83% and ~91% of the theoretical capacities, respectively. Two subsequent desorption cycles were performed after rehydrogenating the sample under 430 bar of hydrogen at 300 °C for 6 hours. The second desorption cycle showed a reduction in the H_2 capacity to 2.7 wt% and the 3rd desorption cycle shows a further decrease in the H_2 capacity to 1.9 wt%. The rate of hydrogen release, Figure 5(b), shows the first desorption cycle is similar in appearance to the TPD-MS measurement, Figure 1(c), but with the H_2 desorption peaks shifted to slightly higher temperatures due to the back-pressure of evolved H_2 ($p(H_2)$ ~ 1.56 bar at 515 °C). The second and third desorption cycles are distinctly different in form to the 1st desorption cycle but are qualitatively similar to each other. In these cases there are main desorption events centred at between 250 and 275 °C with two smaller desorption events occurring just above 400 °C. The slight decrease in the temperature of the H_2 desorption peaks for the 3rd cycle can most likely be attributed to the smaller amount of sample used in this measurement and the lower hydrogen pressure evolved.

To gain an insight into the rehydriding process, *ex situ* XRD was performed on samples after the application of various desorption and absorption conditions, Figure 6. Figure 6(a) shows the *ex situ* XRD pattern of the 6KAlH$_4$-Al$_2$S$_3$ sample from Figure 5(a) that had been cooled under its own evolved hydrogen pressure after decomposition at 515°C. Only peaks from KAlS-4 and Al can readily be identified. The *in situ* SXRD performed under vacuum, Figure 1(b), showed that KAlS-4 disappeared between ~370 and 425°C with the corresponding appearance of KAlS-5. The presence of KAlS-4 observed at room-temperature after TPD measurements up to 515 °C is further evidence of a reversible solid-state phase transition between KAlS-4 and KAlS-5. Figure 6(b) shows a 6KAlH$_4$-Al$_2$S$_3$ sample hydrided for 6 h at a temperature of 300 °C and 430 bar of H_2 pressure after having previously been decomposed at 500 °C. This revealed that KAlH$_4$ was regenerated after the hydriding process but that the other starting reagent, Al$_2$S$_3$, was not. In fact, no sulphur containing compounds could be identified while a significant quantity of Al metal and two weak peaks (q ~ 2.178 and 2.575 Å^{-1}, d ~ 2.884 and 2.440 Å) from an unidentified phase were also present. If the two weak peaks are excluded then from Rietveld refinement the mass fraction of KAlH$_4$ and Al in the rehydrided product was 0.543 and 0.456, respectively. This corresponds to a molar ratio of KAlH$_4$ to Al of 1:2.18 (±0.04). If KAlH$_4$ was responsible for all the H_2 released during the 3rd desorption then the molar ratio of KAlH$_4$ to Al would need to be 1:1.87. This means that to account for the observed hydrogen release during the third desorption cycle there must be another hydrogen containing phase in the unknown phase or in an amorphous phase. This strongly suggests that the absorption process does not follow the original desorption process and that the reversible capacity may be substantially improved by adjusting the ratio of the starting reagents to minimise the amount of inactive Al. Additional research into the impact of molten phases formed during desorption under H_2 pressure is also required. Segregation of products in the molten phase could contribute to a reduction in H_2 capacity but, in some cases, hydriding above the melting point improves reversibility. For example, starting from Na, Al and gaseous H_2, the original uncatalysed formation of NaAlH$_4$ was performed at temperatures above its melting point [68].

In contrast to a decomposed 6KAlH$_4$-Al$_2$S$_3$ sample hydrided at 300 °C and $p(H_2)$ = 430 bar, samples rehydrided at lower pressures, T = 300 °C and $p(H_2)$ = 80 or 107 bar, were almost entirely composed of the unknown phase KAlS-2 and Al, Figure 6(c). Only two small peaks positioned at q ~ 2.006 and 2.540 Å^{-1} (d = 3.132 and 2.474 Å, respectively), could not be identified. After 4 cycles of hydrogen release and uptake, utilising T = 300 °C and $p(H_2)$ = 80 bar for absorption, the hydrided sample, Figure 6(d), showed noticeable changes in the products formed compared to those observed after the first absorption cycle. In addition to the KAlS-2 phase, the room-temperature rhombohedral polymorph of KHS (space group: R-3m, hexagonal setting, stable up to 148 °C) [61] was present in addition to unidentified peaks located at q ~ 1.135, 2.268 and 2.569 Å^{-1} (d = 5.536, 2.770 and 2.446 Å). Based on the reported enthalpies of desorption for KAlH$_4$ (ΔH_{des} = 70 kJ/mol·H_2 for Eq. 1; ΔH_{des} =

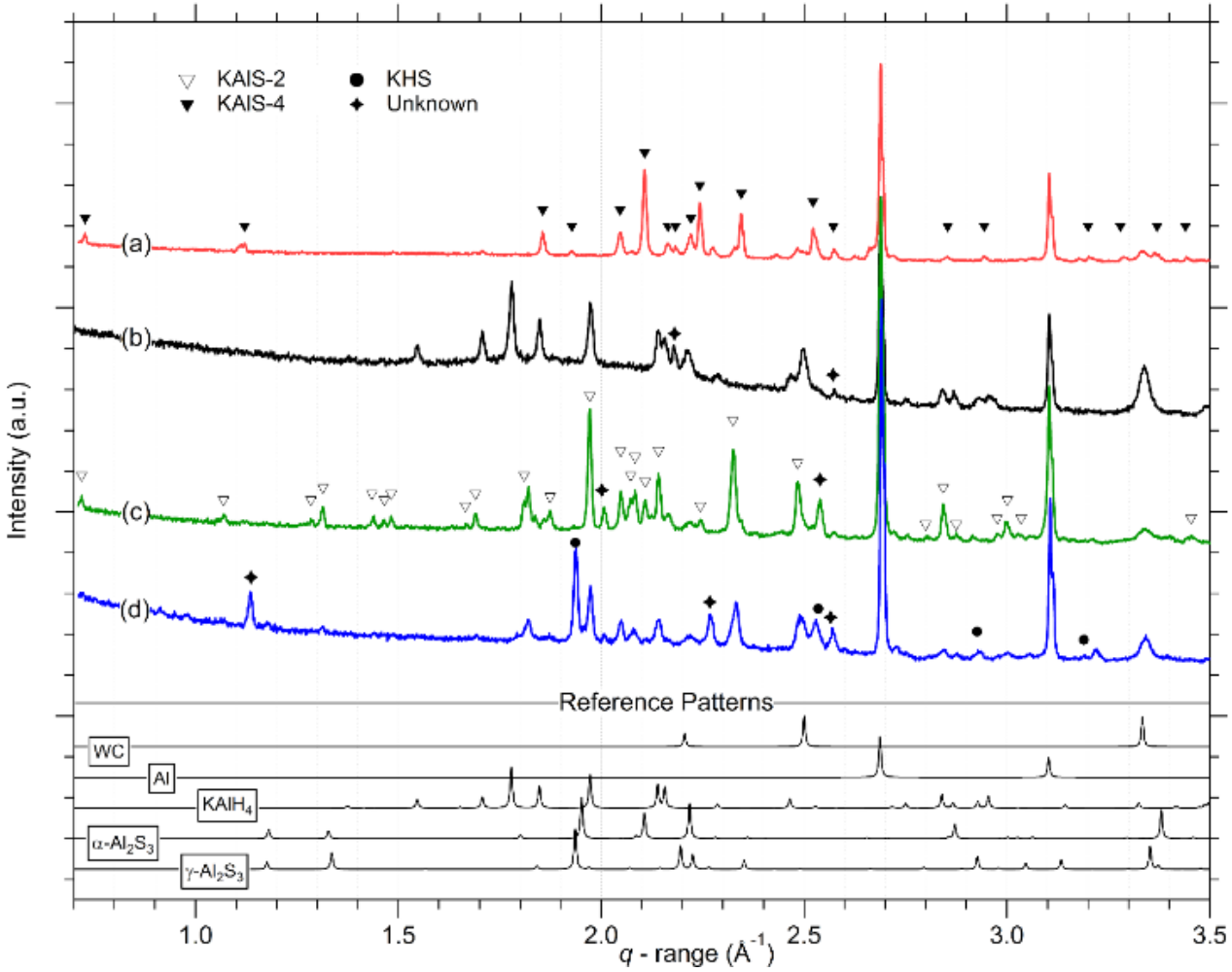

Figure 6: X-ray diffraction patterns of: (a) the 6KAlH$_4$-Al$_2$S$_3$ sample after TPD to 500 °C in a closed Sieverts instrument that began under static vacuum and was cooled under its evolved hydrogen pressure; (b) a decomposed sample of 6KAlH$_4$-Al$_2$S$_3$, using the sample conditions as (a), that was rehydrided for 6 h at T = 300 °C and p(H$_2$) = 430 bar; (c) the sample from (a) that was hydrided for 10 h at T = 300 °C and p(H$_2$) = 80 bar; (d) the sample from (a) after the 4th hydriding at T = 300 °C and p(H$_2$) = 80 bar.

81 kJ/mol·H$_2$ for Eq. 2) and the entropies of desorption (ΔS_{des} = 128.7 J/mol·H$_2$·K for Eq. 1; ΔS_{des} = 128.1 J/mol·H$_2$·K for Eq. 2) derived from the reported H$_2$ equilibrium plateau pressures at 355 °C [51], the corresponding H$_2$ equilibrium pressures at 300 °C for the KAlH$_4$ decomposition reactions corresponding to Eq. 1 and Eq. 2 were calculated as ~2.2 and 0.2 bar, respectively. Due to the fact that the final decomposition reaction products could only be rehydrided to KAlS-2 using 107 bar of H$_2$ pressure at 300 °C, and that a pressure of 430 bar of H$_2$ at this temperature was required to regenerate KAlH$_4$, indicates that Al$_2$S$_3$ successfully acts as a thermodynamic destabilising agent. The hydrogen absorption conditions used also provide boundaries for the reaction enthalpy between KAlH$_4$ and the products of KAlS-2 and Al. If the entropy is assumed to be similar to that for pure KAlH$_4$ decomposition, ΔS_{abs} = -128 J/mol·H$_2$·K, then $\Delta H_{des} = T{\cdot}\Delta S_{abs} - R{\cdot}T{\cdot}\ln(P_o/P_{abs})$, where R = 8.3145 J/mol·K. Using a temperature of 573.15 K (300 °C) and H$_2$ pressures of 107 and 430 bar, respectively, results in ΔH_{abs} between -44.5 and -51.1 kJ/mol·H$_2$.

Conclusions

The reaction mechanism for hydrogen release and uptake of potassium alanate, KAlH$_4$, was successfully changed by the addition of Al$_2$S$_3$ and the formation of KH and molten K avoided. This work reveal new opportunities to release all of the hydrogen in the composite, increase the hydrogen capacity and optimise the thermodynamic properties. Similar to the 6NaAlH$_4$-Al$_2$S$_3$ system, the decomposition of 6KAlH$_4$-Al$_2$S$_3$ occurred through a number of previously unknown compounds but, unlike the 6NaAlH$_4$-Al$_2$S$_3$ system, the final decomposition products were not an alkali metal sulphide and aluminium metal. During heating up to 515 °C, the 6KAlH$_4$-Al$_2$S$_3$ system released ~92 % of the theoretical hydrogen capacity but subsequent desorption cycles showed reduced capacity and a change in the decomposition pathways. Analysis of the rehydrided material showed a large excess of metallic aluminium that indicates that reversible hydrogen capacity can be improved through optimisation of the starting reagent ratios. Heating 6KAlH$_4$-Al$_2$S$_3$ under a hydrogen atmosphere showed that the intermediate decomposition product, denoted KAlS-2, underwent melting in the temperature range 300 to 350 °C and the effect this molten phase has on the reversibility of the system requires further investigation. Moreover,

decomposition of $6KAlH_4$-Al_2S_3 during heating under dynamic vacuum began at 185 °C, which is 65 °C lower than for pure $KAlH_4$, and released 71% of the theoretical hydrogen content below 300 °C. The hydrogen release occurred through multiple unknown compounds. Despite some unknown crystalline compounds, the reversibility of hydrogen release shows promise for technical applications. Unlike the $6NaAlH_4$-Al_2S_3 system, the $6KAlH_4$-Al_2S_3 system did not have M_3AlH_6 (M = alkali metal) as one of the intermediate decomposition products nor were the final products M_2S and Al observed. Decomposition performed under hydrogen pressure initially followed a similar reaction pathway to that observed during heating under vacuum but resulted in partial melting of the sample between 300 and 350 °C. Although, the hydrogen capacity decrease during consecutive H_2 release and uptake cycles, the presence of excess amounts of aluminium allow for further optimisation hydrogen storage properties. The measured enthalpy of hydrogen absorption (ΔH_{abs}) was in the range -44.5 to -51.1 kJ/mol·H_2, which is favourable for moderate temperature hydrogen applications. This study has revealed the complexity of sulphur chemistry during interactions with alkali metals and hydrogen and simultaneously open new prospects for optimisation of the present alanate-aluminium sulphide type composite and design and discovery of novel types of reactive hydride composites.

Conflicts of interest

There are no conflicts to declare.

Acknowledgements

The authors acknowledge the financial support of the Australian Research Council (ARC) for ARC Linkage grant LP120101848, LP150100730 and Future Fellowship FT160100303. D.A.S would also like to acknowledge a Curtin University Early Career Research Fellowships for financial support. The Innovation foundation Denmark, via the project *HyFillFast*, the Danish National Research Foundation, via the Center for Materials Crystallography (DNRF93) and the Danish council for independent research, technology and production, via HyNanoBorN (DFF – 4181-00462) are acknowledged for financial support. We are also grateful to the SWNBL the beamline ID22 at ESRF, Grenoble, France and the beamline I711 at MAXlab, Lund, Sweden for the provision of beamtime.

Notes and references

1. M. Hirscher, ed., *Handbook of Hydrogen Storage: New Materials for Future Energy Storage*, Wiley-VCH Verlag GmbH & Co. KGaA, Weinheim, 2010.
2. S. Garroni, A. Santoru, H. Cao, M. Dornheim, T. Klassen, C. Milanese, F. Gennari and C. Pistidda, *Energies*, 2018, **11**, 1027.
3. L. H. Jepsen, M. B. Ley, Y.-S. Lee, Y. W. Cho, M. Dornheim, J. O. Jensen, Y. Filinchuk, J. E. Jørgensen, F. Besenbacher and T. R. Jensen, *Materials Today*, 2014, **17**, 129-135.
4. M. Paskevicius, L. H. Jepsen, P. Schouwink, R. Cerny, D. B. Ravnsbaek, Y. Filinchuk, M. Dornheim, F. Besenbacher and T. R. Jensen, *Chemical Society Reviews*, 2017, **46**, 1565-1634.
5. Y. Wang and Y. Wang, *Progress in Natural Science: Materials International*, 2017, **27**, 41-49.
6. X. Zhang, Z. Ren, X. Zhang, M. Gao, H. Pan and Y. Liu, *Journal of Materials Chemistry A*, 2019, **7**, 4651-4659.
7. B.-X. Dong, L. Wang, J. Ge, C. Ping, Y.-L. Teng and Z.-W. Li, *Physical Chemistry Chemical Physics*, 2018, **20**, 11116-11122.
8. K. T. Møller, M. Jørgensen, J. G. Andreasen, J. Skibsted, Z. Łodziana, Y. Filinchuk and T. R. Jensen, *Int. J. Hydrogen Energy*, 2018, **43**, 311-321.
9. M. B. Ley, L. H. Jepsen, Y.-S. Lee, Y. W. Cho, J. M. Bellosta von Colbe, M. Dornheim, M. Rokni, J. O. Jensen, M. Sloth, Y. Filinchuk, J. E. Jørgensen, F. Besenbacher and T. R. Jensen, *Materials Today*, 2014, **17**, 122-128.
10. M. Matsuo and S.-i. Orimo, *Adv. Energy Mater.*, 2011, **1**, 161-172.
11. B. R. S. Hansen, M. Paskevicius, H.-W. Li, E. Akiba and T. R. Jensen, *Coordination Chemistry Reviews*, 2016, **323**, 60-70.
12. P. E. de Jongh, D. Blanchard, M. Matsuo, T. J. Udovic and S. Orimo, *Appl. Phys. A*, 2016, **122**, 251.
13. Y. Oumellal, A. Rougier, G. A. Nazri, J. M. Tarascon and L. Aymard, *Nature Materials*, 2008, **7**, 916-921.
14. S. Sartori, F. Cuevas and M. Latroche, *Appl Phys a-Mater*, 2016, **122**, 135.
15. L. Aymard, Y. Oumellal and J. P. Bonnet, *Beilstein Journal of Nanotechnology*, 2015, **6**, 1821-1839.
16. K. Møller, D. Sheppard, D. Ravnsbæk, C. Buckley, E. Akiba, H.-W. Li and T. Jensen, *Energies*, 2017, **10**, 1645.
17. R. Mohtadi and S.-i. Orimo, *Nature Reviews Materials*, 2016, **2**.
18. P. Schouwink, E. Didelot, Y.-S. Lee, T. Mazet and R. Černý, *Journal of Alloys and Compounds*, 2016, **664**, 378-384.
19. P. Schouwink, M. B. Ley, A. Tissot, H. Hagemann, T. R. Jensen, Ľ. Smrčok and R. Černý, *Nature Communications*, 2014, **5**, 5706.
20. B. Bogdanović and B. Spliethoff, *Zeitschrift für physikalische Chemie, Neue Folge*, 1989, **164**, 1497-1508.
21. B. Bogdanović, A. Ritter, B. Spliethoff and K. Straburger, *Int. J. Hydrogen Energy*, 1995, **20**, 811-822.
22. A. Reiser, B. Bogdanovic and K. Schlichte, *Int. J. Hydrogen Energy*, 2000, **25**, 425-430.
23. M. Felderhoff and B. Bogdanović, *International Journal of Molecular Sciences*, 2009, **10**, 325-344.
24. D. A. Sheppard, M. Paskevicius and C. E. Buckley, *Chem. Mater.*, 2011, **23**, 4298-4300.
25. D. A. Sheppard, C. Corgnale, B. Hardy, T. Motyka, R. Zidan, M. Paskevicius and C. E. Buckley, *RSC Adv.*, 2014, **4**, 26552-26562.
26. D. A. Sheppard, M. Paskevicius, T. D. Humphries, M. Felderhoff, G. Capurso, J. Bellosta von Colbe, M. Dornheim, T. Klassen, P. A. Ward, J. A. Teprovich, C. Corgnale, R. Zidan, D. M. Grant and C. E. Buckley, *Appl. Phys. A*, 2016, **122**, 395.
27. D. A. Sheppard, T. D. Humphries and C. E. Buckley, *Applied Physics A*, 2016, **122**, 406.
28. T. D. Humphries, D. A. Sheppard, M. R. Rowles, M. V. Sofianos and C. E. Buckley, *J. Mater. Chem. A*, 2016, **4**, 12170-12178.

29. M. S. Tortoza, T. D. Humphries, D. A. Sheppard, M. Paskevicius, M. R. Rowles, M. V. Sofianos, K. F. Aguey-Zinsou and C. E. Buckley, *Physical Chemistry Chemical Physics*, 2018, **20**, 2274-2283.
30. E. Rönnebro, G. Whyatt, M. Powell, M. Westman, F. Zheng and Z. Fang, *Energies*, 2015, **8**, 8406-8430.
31. P. A. Ward, C. Corgnale, J. A. Teprovich, T. Motyka, B. Hardy, D. Sheppard, C. Buckley and R. Zidan, *Applied Physics A*, 2016, **122**, 462.
32. M. V. Lototskyy, I. Tolj, L. Pickering, C. Sita, F. Barbir and V. Yartys, *Progress in Natural Science: Materials International*, 2017, **27**, 3-20.
33. K. T. Møller, T. R. Jensen, E. Akiba and H.-w. Li, *Progress in Natural Science: Materials International*, 2017, **27**, 34-40.
34. Y. Yan, H.-W. Li, H. Maekawa, K. Miwa, S.-i. Towata and S.-i. Orimo, *The Journal of Physical Chemistry C*, 2011, **115**, 19419-19423.
35. M. Paskevicius, B. R. S. Hansen, M. Jorgensen, B. Richter and T. R. Jensen, *Nature Communications*, 2017, **8**, 15136.
36. T. Inada, T. Kobayashi, N. Sonoyama, A. Yamada, S. Kondo, M. Nagao and R. Kanno, *Journal of Power Sources*, 2009, **194**, 1085-1088.
37. N. Kamaya, K. Homma, Y. Yamakawa, M. Hirayama, R. Kanno, M. Yonemura, T. Kamiyama, Y. Kato, S. Hama, K. Kawamoto and A. Mitsui, *Nature Materials*, 2011, **10**, 682-686.
38. A. Unemoto, T. Ikeshoji, S. Yasaku, M. Matsuo, V. Stavila, T. J. Udovic and S.-i. Orimo, *Chemistry of Materials*, 2015, **27**, 5407-5416.
39. S. Zaman and K. J. Smith, *Catalysis Reviews*, 2012, **54**, 41-132.
40. N. Koizumi, K. Murai, T. Ozaki and M. Yamada, *Catalysis Today*, 2004, **89**, 465-478.
41. W. Wang, S. Wang, X. Ma and J. Gong, *Chemical Society Reviews*, 2011, **40**, 3703-3727.
42. M. Paskevicius, B. Richter, M. Polanski, S. P. Thompson and T. R. Jensen, *Dalton Trans*, 2016, **45**, 639-645.
43. J. M. Lalancette and A. Frêche, *Canadian Journal of Chemistry*, 1969, **47**, 739-742.
44. H. Firouzabadi, B. Tamami and A. R. Kiasat, *Phosphorus, Sulfur, and Silicon and the Related Elements*, 2000, **159**, 99-108.
45. M. B. Smith and G. E. Bass Jr., *Journal of Chemical and Engineering Data*, 1963, **8**, 342-346.
46. A. Roine, *HSC Chemistry*, 2006.
47. D. D. Wagman, W. H. Evans, V. B. Parker, R. H. Schumm, I. Halow, S. M. Bailey, K. L. Churney and R. L. Nutall, *Journal of Physical and Chemical Reference Data*, 1982, **11, Suppl. 2**.
48. K. S. Gavrichev, *Inorganic Materials*, 2003, **39**, S89-S112.
49. M. Mamatha, C. Weidenthaler, A. Pommerin, M. Felderhoff and F. Schüth, *Journal of Alloys and Compounds*, 2006, **416**, 303-314.
50. L. M. Arnbjerg and T. R. Jensen, *Int. J. Hydrogen Energy*, 2012, **37**, 345-356.
51. J. R. Ares, K.-F. Aguey-Zinsou, F. Leardini, I. J. m. Ferrer, J.-F. Fernandez, Z.-X. Guo and C. Sánchez, *J. Phys. Chem. C*, 2009, **113**, 6845-6851.
52. D. A. Sheppard, L. H. Jepsen, T. R. Jensen, M. Paskevicius and C. E. Buckley, *J. Mater. Chem. A*, 2013, **1**, 12775-12781.
53. B. R. S. Hansen, K. T. Møller, M. Paskevicius, A.-C. Dippel, P. Walter, C. J. Webb, C. Pistidda, N. Bergemann, M. Dornheim, T. Klassen, J.-E. Jørgensen and T. R. Jensen, *Journal of Applied Crystallography*, 2015, **48**, 1234-1241.
54. M. Paskevicius, M. B. Ley, D. A. Sheppard, T. R. Jensen and C. E. Buckley, *Phys. Chem. Chem. Phys.*, 2013, **15**, 19774-19789.
55. M. B. Ley, M. Paskevicius, P. Schouwink, B. Richter, D. A. Sheppard, C. E. Buckley and T. R. Jensen, *Dalton Trans.*, 2014, **43**, 13333-13342.
56. E. Roedern, B. R. S. Hansen, M. B. Ley and T. R. Jensen, *J. Phys. Chem. C*, 2015, **119**, 25818-25825.
57. E. M. Dematteis, E. Roedern, E. R. Pinatel, M. Corno, T. R. Jensen and M. Baricco, *RSC Advances*, 2016, **6**, 60101-60108.
58. T. T. Nguyen, D. A. Sheppard and C. E. Buckley, *Journal of Alloys and Compounds*, 2017, **716**, 291-298.
59. E. C. Ashby, *Chemical and Engineering News*, 1969, **47**, 9.
60. F. Haarmann, H. Jacobs and W. Kockelmann, *The Journal of Chemical Physics*, 2000, **113**, 6788.
61. F. Haarmann, H. Jacobs, J. Senker and E. Rössler, *The Journal of Chemical Physics*, 2002, **117**, 1269.
62. E. E. Hellstrom and R. A. Huggins, *Materials Research Bulletin*, 1979, **14**, 881-889.
63. R. Černý and Y. Filinchuk, *Zeitschrift für Kristallographie*, 2011, **226**, 882-891.
64. A. A. Coelho, *Journal of Applied Crystallography*, 2018, **51**, 210-218.
65. J.-H. Shim, J.-H. Lim, S.-u. Rather, Y.-S. Lee, D. Reed, Y. Kim, D. Book and Y. W. Cho, *Journal of Physical Chemistry Letters*, 2010, **1**, 5.
66. K. B. Kim, J. H. Shim, Y. W. Cho and K. H. Oh, *Chemical Communications*, 2011, **47**, 9831-9833.
67. B. Bogdanovic, A. Reiser, K. Schlichte, B. Spliethoff and B. Tesche, *J. Alloys Compd.*, 2002, **345**, 77-89.
68. T.N. Dymova, N.G. Eliseeva, S.I. Bakum and Yu. M. Dergachev, *Doklady Akademii Nauk SSSR*, 1974, **215**, Engl. 256.